iVES OENO One vine & wine

DOI: https://doi.org/10.20870/oeno-one.2025.59.4.8461

OPEN ACCESS

VITICULTURE ORIGINAL RESEARCH ARTICLES

Exploring soil–plant interactions in vineyards using geophysics and hyperspectral imaging

Maxime Lavaud[1,2], Myriam Schmutz[3,4,*], Jehanne Cavailhes[3], Nicola Falco[4]

[1] Univ. Bordeaux, CNRS, LOMA, UMR 5798, F-33400 Talence, France
[2] Univ. Bordeaux, CNRS, Bordeaux INP, CBMN, UMR 5248, F-33600 Pessac, France
[3] Univ. Bordeaux, CNRS, Bordeaux INP, EPOC, UMR 5805, F-33400 Talence, France
[4] Lawrence Berkeley National Laboratory, Berkeley, CA 94720, USA

Article number: 8461

*correspondence:
myriam.schmutz@ipb.fr

Associate editor:
Amélie Quiquerez

Received:
2 January 2025

Accepted:
22 July 2025

Published:
17 October 2025

This article is published under the **Creative Commons licence** (CC BY 4.0).

Use of all or part of the content of this article must mention the authors, the year of publication, the title, the name of the journal, the volume, the pages and the DOI in compliance with the information given above.

ABSTRACT

Climate change and evolving land management practices are reshaping soil–plant interactions critical for sustainable viticulture. These interactions are driven by soil texture, hydrogeochemical gradients, and climatic conditions, influencing grapevine traits like nutrient and water content. Integrating innovative methods, this study explores the relationship between soil variability and grapevine characteristics in the Médoc wine region, France.

The research combines hyperspectral imaging, electromagnetic induction (EMI), and electrical resistivity tomography (ERT) with traditional soil and leaf sampling. Hyperspectral data, using visible-near infrared (VNIR) wavelengths, reliably estimated leaf traits such as nitrogen and water content, yielding strong predictive relationships (R^2 up to 0.8). These findings suggest VNIR-based indices are cost-effective for monitoring grapevine physiology.

Geophysical data revealed significant soil textural gradients, delineating sand, transitional (loam, sandy loam), and clay textural soil classes. Apparent electrical conductivity (ECa) and inverted electrical conductivity (EC) correlated with soil texture and grapevine traits, particularly at depths around 50 cm, aligning with primary root zones. However, interannual variability in correlations emphasised the influence of weather conditions and phenological stages, highlighting the need to align data acquisition with vine growth phases.

The integration of hyperspectral imaging and geophysical methods provides a novel framework for linking soil and plant parameters. This interdisciplinary approach enhances the spatial resolution and scalability of vineyard monitoring, offering actionable insights for precision viticulture. Future work should expand datasets and refine predictive models to improve the understanding of soil–plant dynamics under changing environmental conditions.

These findings underscore the potential of combining hyperspectral and geophysical data to develop climate-resilient vineyard management strategies, advancing precision agriculture, and sustainable viticulture practices.

KEYWORDS: precision viticulture, soil electrical conductivity, hyperspectral, soil–plant interactions, spatial variability, leaf nitrogen, water content

INTRODUCTION

Global challenges posed by climate change, wildfires, extreme weather events, and evolving land management practices are transforming the intricate interplay between soil, microbes, plants, and climate. These interactions are fundamental to water and nutrient cycles that directly influence agricultural productivity (Pugnaire *et al.*, 2019). In viticulture, these dynamics are further shaped by soil texture, hydrogeochemical gradients, and climatic conditions, with profound implications for vineyard sustainability. Addressing these challenges requires the wine industry to adopt innovative, climate-resilient management strategies ensuring long-term viability (Ammoniaci *et al.*, 2021; Fuentes & Gago, 2022).

Understanding soil–plant interactions is central to achieving such resilience. Traditionally, these interactions have been studied separately within the biosphere and geosphere using distinct methodologies. Within the biosphere, grapevine variability has been assessed through direct methods, such as pruning weights or Leaf Area Index (LAI) measurements (Anderson *et al.*, 2004), and indirect approaches like remote sensing. Spectral indices, such as the Normalized Difference Vegetation Index (NDVI), derived from high-resolution imagery, enable non-invasive evaluation of grapevine vigour and LAI (Johnson *et al.*, 2003; Das *et al.*, 2015). Emerging hyperspectral techniques extend these capabilities, enabling precise retrieval of plant nutrient levels like nitrogen (Chadwick *et al.*, 2020), which critically influence grapevine growth, yield, and quality (Darra *et al.*, 2021). As demonstrated by Peanusaha *et al.* (2024), machine learning applied to full-spectrum hyperspectral data outperforms traditional regression models based on vegetation indices. This improvement stems from leveraging the rich, high-resolution spectral information now available, even if challenges persist due to variability in spectral responses across environmental conditions and phenological stages (Moghimi *et al.*, 2020).

Machine learning advancements, such as random forest modelling, further enhance the accuracy and transferability of spectral data for estimating nitrogen and other plant traits (Berger *et al.*, 2020; Yu & Kurtural, 2020). These models handle nonlinear relationships, outliers, and complex interactions between variables (Yu *et al.*, 2021). Their findings underscore the advantages of raw spectral data over index-based maps, particularly when combining hyperspectral and electromagnetic (EM) data to assess soil water concentration.

Simultaneously, the geosphere is characterised through soil sampling, profile methods, which, while detailed, are spatially limited and labour-intensive (Brevik *et al.*, 2016). Advances in geophysical techniques, especially Electrical Resistivity Tomography (ERT) and electromagnetic induction (EMI), have transformed non-invasive soil characterisation (van Leeuwen *et al.*, 2024; and references therein). The application of EMI in viticulture is supported by an extensive body of research demonstrating its ability to delineate homogeneous soil units and provide critical insights into soil variability at high spatial resolution (Martini *et al.*, 2013; Bonfante *et al.*, 2015; Pradipta *et al.*, 2022). In addition, numerous studies have explored the use of geophysical instruments, including EMI and ERT, for soil mapping and monitoring in vineyards, highlighting their potential to enhance precision viticulture strategies (van Leeuwen, 2021). Likewise, the increasing availability of drone-based multispectral and hyperspectral imaging has significantly improved our capacity to assess vineyard heterogeneity, with a wealth of literature documenting its effectiveness in monitoring vine health and vigour (Sarri *et al.*, 2019; Pradipta *et al.*, 2022).

While the individual applications of hyperspectral imaging, geophysical surveys, soil sampling, and leaf trait measurements have been extensively investigated, a comprehensive integration of these approaches remains largely unexplored. Moreover, the quasi-3D inversion of EMI conductivity data, which could significantly refine our understanding of soil–plant interactions, has yet to be fully leveraged in viticulture. To address these gaps, this study explores the relationship between soil properties (*e.g.*, texture, water content) and grapevine leaf traits, including nutrient and water status.

By leveraging machine learning techniques and integrating geophysical and hyperspectral datasets, we aim to advance predictive modelling and optimise climate-resilient vineyard management strategies. Ultimately, our approach highlights the benefits of multi-scale, data-driven methodologies for enhancing vineyard sustainability in the face of evolving environmental and agronomic challenges.

MATERIALS AND METHODS

1. Study area

The study area is situated in the Médoc wine region, located in the north of Bordeaux, France, renowned for its historic viticulture and world-famous red wines. The region is characterised by gravel-rich soils, known as *peyrosols*, which provide optimal drainage and heat retention, fostering ideal vine growth conditions. The Atlantic Ocean moderates the local climate, resulting in mild temperatures (annual mean of 12.7 °C) and a growing season with a balanced water supply. Forested areas surrounding vineyards contribute to thermal regulation. However, viticulture in the region faces challenges, particularly fungal diseases such as mildew and rot, which necessitate the widespread use of copper-based fungicides.

The specific study plot exhibits a minimal topographical variation, with an elevation range of 3.2 m, and is characterised by shallow soil horizons overlying calcareous clay layers encountered at depths generally exceeding 1.5 m. Soil characterisation was performed through the excavation of seven pits, which revealed that the rooting depth of Merlot grapevines is predominantly limited to the upper 1.5 m. This rooting restriction is attributed to the presence of dense clay layers and a shallow water table, both acting as barriers to deeper root development. These conditions underscore the plot's unique terroir characteristics.

2. Leaf sampling

In 2022, leaf sampling was conducted at 30 stations, with approximately 120 leaves collected at four orientations (north, south, east, and west) on each plant. In 2023, sampling was extended to 45 stations, with 30 stations remaining comparable to 2022. Six leaves at varying stages of maturity were collected per station in 2023, resulting in a total of 270 leaves. Leaves were immediately sealed in airtight bags and transported to the laboratory.

Laboratory analyses included:

- Quantification of total nitrogen, potassium, and carbon using combustion via the Dumas method (NF EN ISO 16634-2, 2016)
- Determination of water content through drying (NF EN ISO 662, 2001).

The data are available in Figure S1.

3. Soil sampling

In 2023, soil samples were collected at a depth of 0.30 m at each of the 45 stations (Figure 1). Due to the soil's compact and gravelly nature, deeper sampling was not feasible. Samples were prepared according to NF EN ISO 11464 and analysed by the Laboratoire Régional de Contrôle des Eaux de Limoges. Analyses included:

- Soil texture determined using granulometric pipetting (NF X31-107, 2003)
- Cation Exchange Capacity (CEC) measured with the Metson method (NF X31-130)
- pH measured instrumentally (NF ISO 10390)
- Potassium content determined using ammonium acetate extraction (NF X31-108)
- Organic matter and nitrogen content assessed by combustion (NF ISO 10694 and NF ISO 13878).

The textural soil sample analysis for the topsoil 45 stations indicates the existence of three zones corresponding to three main classes following the USDA classification: sand class (37/45), clay class (5/45), and transitional zone combining loam and sandy loam (3/45). The data are available in Figure S1.

4. Geophysical survey

4.1. Apparent resistivity maps acquisition

Electromagnetic induction (EMI) surveys were performed using the CMD Mini-Explorer device (GF Instrument, Czech Republic) with a transmission frequency of 30 kHz. The device comprises one transmitter and three receiver coils, in both vertical and horizontal coil orientations (HCP and VCP). Each orientation allows for three different depths of investigation: VCP corresponds to 0–0.25; 0–0.7; 0–1.5, and HCP to 0–0.5; 0–1; 0–2 m, leading to a combination of measurements for six investigation depths. Two successive campaigns of apparent conductivity (ECa) measurements were acquired:

- 2022: manual measurements were taken every 5 m along rows, spaced approximately 5 m apart; and
- 2023: measurements were acquired continuously along the same rows.

Data were georeferenced using a Differential Global Positioning System (DGPS). The apparent conductivity values are obtained with the Low Induction Number (LIN) model (McNeill, 1980), and processed to remove noise from metal objects (*e.g.*, trellis wires) and outlier values (> 100 mS/m or < 0 mS/m). Data collected from soil and leaf samples are available in Figure S1.

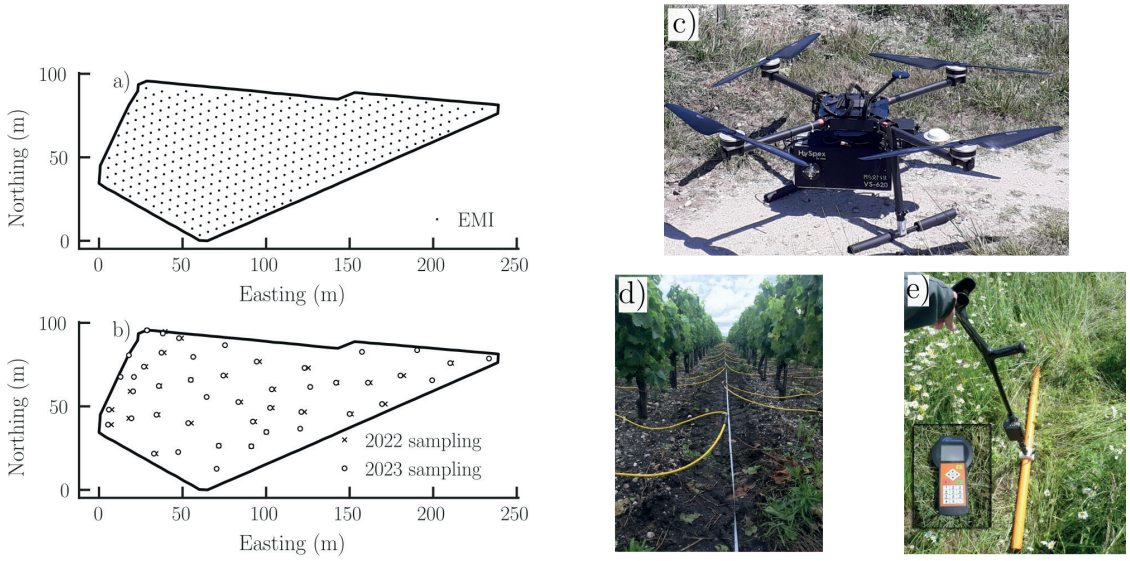


FIGURE 1. a) Location of EMI measurement stations in point mode, b) location of leaf and soil sampling, and pictures of c) the drone used for airborne hyperspectral data acquisition system, d) the ERT acquisition system, and e) the EMI acquisition system.

4.2. Inverted resistivity transects

To get reliable information concerning vertical and horizontal soil geometry variation, Electrical Resistivity Tomography (ERT) was acquired with an MPT DAS-1 system, both with 0.5 and 1 m electrode interspace, respectively, over 31.5 and 71 m long profiles. The 2D electrical resistivity inversion process, providing 2D images of inverted electrical resistivity from apparent resistivities, was done with Res2Dinv software (Loke, 2004). The inversion R^2 is 1.5 % for each profile. The ERT profiles were also used to calibrate the ECa EMI maps (McLachlan *et al.*, 2021).

4.3. Pseudo-3D EC EMI inversion

To better apprehend soil geometry and heterogeneity laterally and vertically over the whole studied parcel, we processed the pseudo-3D inversion of all the ECa data obtained with the six depths of investigation calibrated by an ERT transect. This inversion had been done using the EMagPy software (McLachlan *et al.*, 2021), using a linear cumulative sensitivity model (McNeill, 1980). McLachlan *et al.* (2021) demonstrated that deviations from the fully 3D model remain small (up to a conductivity of 100 mS/m) when measurements are taken close to the ground surface (see Figure 5 in McLachlan *et al.*, 2021). Under these conditions, the LIN approximation may slightly underestimate ECa values, but does so systematically and consistently. This justifies the use of the measured values for quasi-3D inversion. Accordingly, we consider it reasonable to present the inverted electrical conductivity parameters in the form of horizontal 2D maps, extending from the topographic surface down to a depth of 1.5 m.

5. Drone-based and ground hyperspectral imaging

Hyperspectral imaging was conducted during the 2022 flowering period using a drone equipped with a Mjolnir-VS620 (HySpex) sensor module. The module collected data across 200 VNIR bands (400–1,000 nm) and 300 SWIR bands (970–2,500 nm).

- Acquisition conditions: measurements were conducted under clear skies to ensure optimal illumination, with spatial resolutions of 3 cm (VNIR) and 6 cm (SWIR); and
- Calibration: images were corrected for atmospheric interference using the ATCOR-4 model, and final outputs included a fused data cube with 422 spectral bands (410.7–2,392.5 nm).

The hyperspectral average reflectance spectrum of classified vine pixels using drone-borne data are represented in Figure 2a.

Ground-based hyperspectral measurements were taken at the same stations as soil and leaf samples using an HR-1024i field spectroradiometer (Spectra Vision Corporation) with

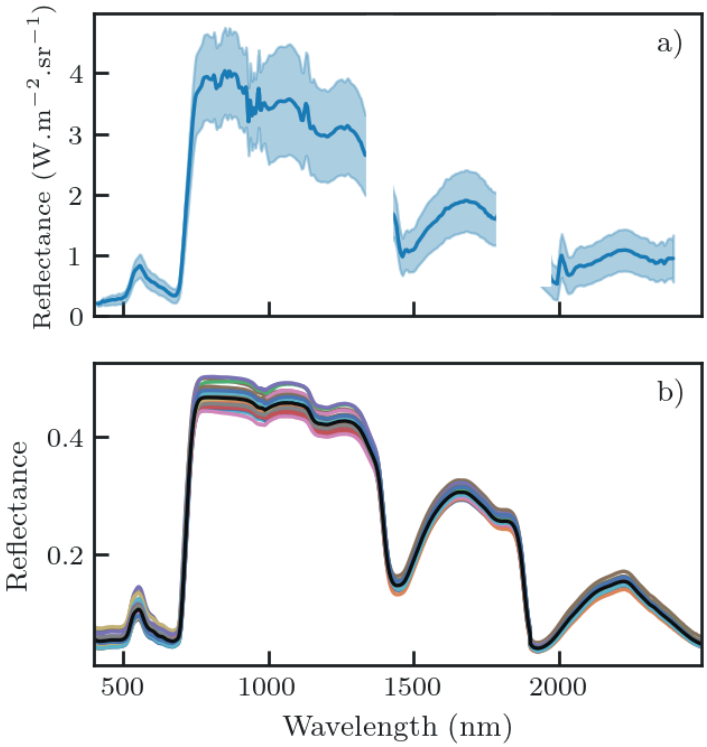


FIGURE 2. Hyperspectral data representation acquired in 2022. a) Average reflectance spectrum of classified vine pixels using drone-borne data. The plain dark blue line corresponds to the average spectrum over the whole field, and the light area lines correspond to the standard deviation. b) Reflectance spectrum of vine leaves measured with a hand spectrometer with respect to a white reference. The black plain line represents the average spectrum over all different locations, and the other colour lines correspond to each sample location.

a spectral range of 250–2,500 nm. Consistent illumination conditions were ensured through a hand-held leaf-clip with its own light source. Measurements were averaged for four leaves in 2022 and six leaves in 2023. The reflectance spectrum of vine leaves measured with a hand spectrometer with respect to a white reference is represented in Figure 2b.

Given that we observe a large deviation on the drone-based data contrary to the hand spectrometer, which can be attributed to the leaf number and orientation on the pixel, we realised a min/max normalisation.

6. Soil zonation analysis

To evaluate the impact of soil textural heterogeneity on soil and vine traits, a geophysical-based soil zoning map was created using *K*-means clustering, built with the sklearn toolbox in Python. The clustering was based on the six raw ECa depths of investigation from the EMI survey. The statistical results combined with our prior knowledge result in three primary soil zones: sand, clay, and a mixture (loam and sandy loam) in the USDA soil classification. This approach builds on methods from McLachlan *et al.* (2022).

7. Regression algorithm to build a predictive model for leaf constituents

To predict leaf traits from drone-based hyperspectral data, we adopted a machine learning approach based on the Random Forest (RF) algorithm over several alternatives, including ordinary least squares, lasso, Ridge regression, support vector machines, and decision trees. Random forest regression, implemented with the Scikit-learn framework in Python. The model's performance was evaluated using leave-one-out cross-validation (LOOCV), a method particularly suited for small datasets. LOOCV ensures the independence of training and testing datasets, thereby reducing the risk of overfitting. This rigorous evaluation protocol allows for reliable assessment of model performance across different configurations. This approach was selected for its ability to handle complex, high-dimensional datasets, such as those combining spectral and geophysical information, while maintaining robustness even with a limited number of samples. RF demonstrated superior robustness and accuracy on our dataset, a performance largely attributable to its use of bootstrapping for generating training sets (*i.e.*, sub-samples with replacement). This characteristic enhances its adaptability to small datasets. The hyperparameters of the RF model, such as maximum tree depth and the number of estimators, were optimised using a random grid search approach.

The dataset used in RF regression integrated three types of information:

- Hyperspectral data: full spectral range or VNIR wavelengths (0.4–1 μm)
- Geophysical data: ECa and EC
- Leaf geochemical analysis: punctual measurements of leaf constituents.

Spatially dense datasets (hyperspectral and geophysical) were smoothed using techniques like the Nadaraya–Watson hat matrix (Ferraty & Vieu, 2006). This preprocessing resulted in eight distinct data configurations, combining spectral ranges (full *vs* VNIR) and data treatment methods (raw *vs* smoothed). The configuration that yielded the highest R^2 score was selected for further analysis.

Our best-performing models achieved R^2 scores ranging from 0.7 to 0.8 with a hand spectrometer, but not applicable for the whole field, and from 0.2 to 0.4 when comparing predicted and measured values using LOOCV. In line with the findings of Ordóñez *et al.* (2013), methods leveraging the full spectral range proved more versatile and reproducible across different studies. These results underline the advantages of incorporating the full spectrum into predictive modelling, despite the increased computational complexity.

It is crucial to avoid directly using observed data for predictions, as this can lead to artificially high R^2 scores, sometimes exceeding 0.8, which are not representative of the model's true performance. Instead, test values must be derived from independent datasets. A limitation of our approach is the relatively small size of the dataset, which restricts the model's applicability to scenarios explicitly represented in the training data. For instance, predictions for new drone-based measurements may not be reliable unless the conditions closely match those of the training dataset.

Nevertheless, the model effectively extends leaf-level data to the airborne scale under similar conditions, providing a practical solution for scaling localised observations. Future research should aim to generalise the model to larger and more diverse datasets to enhance its applicability while maintaining accuracy.

RESULTS AND DISCUSSION

This study presents an innovative integration of leaf chemistry, hyperspectral imaging (handheld and drone-based), and geophysical measurements in vineyards. While this combination is unprecedented, extensive literature supports the relationship between leaf traits, primarily water and nitrogen content, and hyperspectral data. These findings not only validate previous research but also highlight the potential of combining advanced imaging techniques with geophysical tools to improve precision viticulture.

1. Mapping leaf traits using drone-based hyperspectral data

In terms of model accuracy, preliminary analyses showed that machine learning using random forest regression consistently achieved higher R^2 values than traditional regression models based on vegetation indices. This analysis covered a broad set of indices from the index database (Henrich *et al.*, 2012). Tables presenting the most strongly correlated indices for both drone-based and ground-based hyperspectral imaging are provided in Tables S1 and S2.

Notably, the most predictive indices differed between the two measurement approaches. This discrepancy likely stems from differences in what each method captures. Ground-based hyperspectral measurements directly record leaf reflectance, while drone-based data may include mixed signals from leaves, branches, soil, or even atmospheric elements, resulting in more complex spectral signatures.

In terms of spectral range selection, the use of the full spectral range yielded the highest R^2 values for most traits, except for potassium. Restricting the analysis to VNIR wavelengths resulted in marginal decreases in R^2 (less than 10 %), suggesting that VNIR sensors alone could be highly effective. These results align with Peanusaha *et al.* (2024), who emphasise the robustness of VNIR-based indices, such as NDVI and NDRE, for monitoring crop nitrogen levels while acknowledging their limitations in sensitivity and saturation. The integration of SWIR data offered limited improvement (less than 10 %), likely due to dataset size and variability constraints, reaffirming that VNIR-focused approaches can offer cost-effective and scalable solutions.

Furthermore, Peanusaha *et al.* (2024) highlight the superiority of machine learning applied to full-spectrum data over traditional regression-based indices. Their work achieved an R^2 of 0.78 for nitrogen estimation by directly linking spectral and biochemical data from individual leaves, which benefits from precise sample matching. Although our study operates on a larger scale with heterogeneous soil and plant conditions, resulting in slightly lower accuracy, it demonstrates the practicality of VNIR-driven methods in real-world vineyard applications.

Field spectrometer measurements exhibited high accuracy in capturing leaf spectra under controlled conditions, minimising environmental interference. This finding corroborates the observations of Peanusaha *et al.* (2024), underscoring the importance of precise spectral acquisition for robust predictions across variable environmental and phenological conditions. Using these data, hyperspectral inversions produced spatial maps of key leaf traits, revealing notable variability across the study area (Figure 3): nitrogen content ranged from 29 % to 36 %, potassium from 9.6 % to 13.2 %, and carbon from 48 % to 58 %, with spatial patterns strongly influenced by soil heterogeneity. For instance, nitrogen levels were lowest in the clay textural class western section of the parcel, a pattern consistent with Guan *et al.* (2022), who demonstrated soil texture's impact on nutrient availability. Leaf water content was comparatively stable (67–69 %), as leaves were selected to be in a consistent state of size, shape, and colour. These results highlight the critical role of hyperspectral imaging in identifying nutrient-related spatial variability.

However, it is important to recognise the inherent limitations of using hyperspectral reflectance data to infer leaf biochemical traits. One key issue lies in the ill-posed nature of the inverse problem: multiple combinations of leaf properties (*e.g.*, structure, pigment, water content) can produce similar spectral signatures, making it challenging to retrieve unique and accurate trait estimates (*i.e.*, Lamsal *et al.*, 2022). In addition, hyperspectral data are sensitive to both internal leaf structure and external environmental conditions, such as light angle, leaf orientation, and canopy structure, which introduce variability unrelated to biochemical composition (Jacquemoud & Ustin, 2019).

Trait estimation is further complicated by species-specific spectral behaviour and intra-leaf heterogeneity. For example, Ge *et al.* (2019) noted that reflectance models trained on one species or functional group may generalise poorly to others, highlighting the need for species-adapted calibration datasets. Moreover, traits such as potassium and phosphorus often exhibit weaker spectral signatures and less direct correlation with optical properties compared to pigments or water content, reducing model reliability (Ustin *et al.*, 2009).

Recent studies also emphasise that the internal anatomical and physiological variability of leaves, including mesophyll structure, vein density, and age, can alter reflectance independently of chemical content (Cavender-Bares *et al.*, 2020). These factors introduce spectral redundancy and complicate trait retrieval, particularly when operating at the canopy or landscape scale, where leaf mixing and shadowing are prevalent.

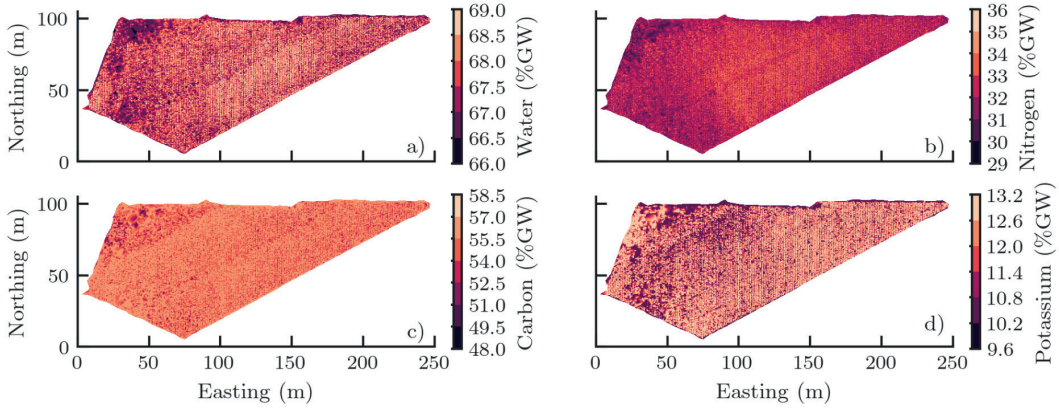


FIGURE 3. Leaf component maps (% GW) derived from the optimal random forest model applied to drone-based hyperspectral data. Maps correspond to: a) water, b) nitrogen, c) carbon, and d) potassium content.

Thus, while hyperspectral imaging provides powerful capabilities for detecting spatial patterns and relative changes in vegetation traits, absolute quantification of specific biochemical components requires cautious interpretation and, ideally, integration with complementary ground-based measurements.

2. Apparent electrical conductivity and inverted electrical conductivity analysis and textural transitions

Apparent electrical conductivity (ECa) mapping, in spite of the fact that they are raw integrative data, is a widely used proxy for defining soil textural variations, particularly in vineyards, as highlighted by the comprehensive review of geophysical methods by van Leeuwen *et al.* (2024). Our study employed a CMD system to acquire ECa data at six investigation depths during the 2022 and 2023 campaigns, offering insights into soil texture across the study site.

ECa values exhibited a clear depth dependency, ranging from 0.7–5 mS/m in shallow layers (Figures 4a and 4b) to 8–40 mS/m in deeper strata (Figures 4e and 4f). Based on these trends, three distinct zones were delineated compatible with USDA soil classification (Figure S1):

1. A sand zone that is resistive in the eastern zone for $X \geq 100$ m;

2. A transitional zone which is composed of loam and sandy loam classes, located at the location $25 < X < 75$ m; and

3. A clay zone that is conductive in the western zone for $X \leq 25$ m.

Inversion results from electrical resistivity tomography (ERT) and electromagnetic induction (EMI) confirmed these textural gradients (Figure 5). Shallow layers (< 2 m) were characterised by sand class soils with high resistivity (≥ 700 Ω m), while deeper layers (> 4 m) displayed low resistivity (< 20 Ω m), indicative of clay substrata. Strong correlations between ERT and EMI-derived ECa values (R^2 = 0.75–0.89) validated the reliability of geophysical measurements in capturing subsurface variability.

These findings align with previous studies, including van Leeuwen *et al.* (2024), who noted that ECa is one of the most extensively studied geophysical parameters in vineyards due to its ease of implementation and strong correlation with soil texture in many contexts. The EMI method, particularly with ARP and EM systems, has proven to be effective in delineating textural variations at shallow depths (~30 cm), as demonstrated by Doolittle *et al.* (1994), Triantafilis and Lesch (2005), and Bonfante *et al.* (2015). However, variations in performance due to factors such as agro-equipment interference, soil compaction, or local heterogeneities have also been reported (Hubbard *et al.*, 2021).

Other and complementary approaches, such as ground-penetrating radar (GPR) and spectral-induced polarisation (SIP), have also shown promise in providing high-resolution soil texture information (*i.e.*, Grote *et al.*, 2010; Revil *et al.*, 2021). Despite their potential, these methods require advanced data processing, making EMI a more practical choice for large-scale applications.

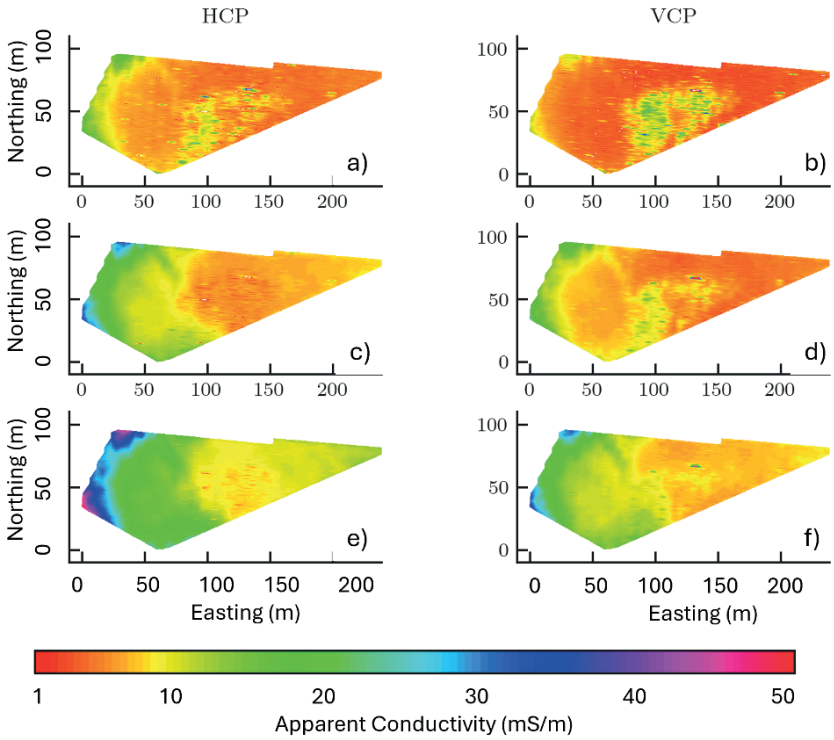


FIGURE 4. ECa maps acquired using a CMD system in HCP and VCP configurations across three coil separations: a, b) 0.32 m, c, d) 0.71 m, e, f) 1.18 m.

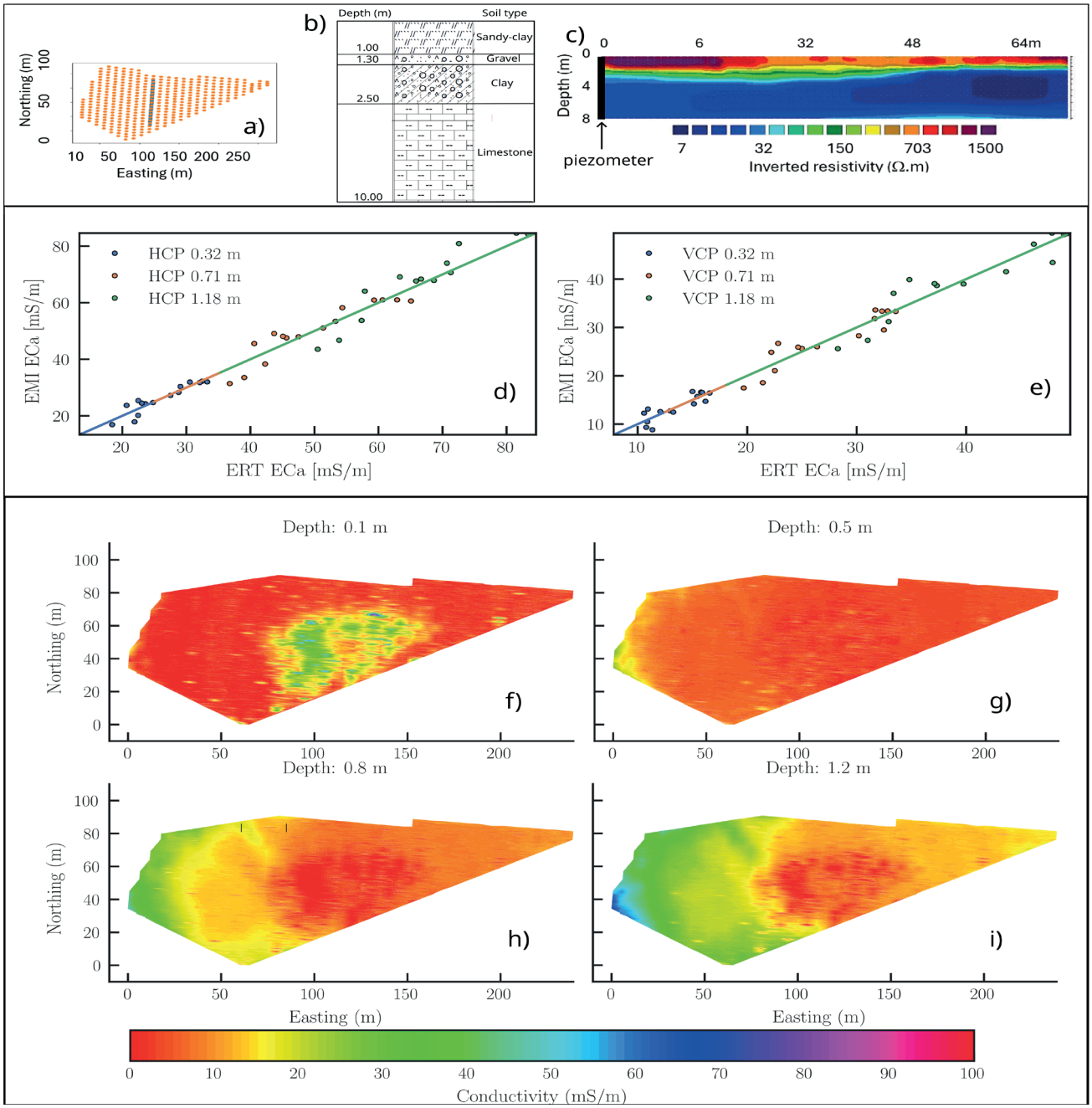


FIGURE 5. a) Location of EMI and ERT measurements; b) Log description of the piezometer located at the ERT origin; c) ERT results; d, e) Calibration of EMI by ERT data for HCP (d) and VCP configurations (e); f to i) Inverted EMI EC maps for depths of (f) 0.1 m, (g) 0.5 m, (h) 0.8 m, and (i) 1.2 m.

In particular, the integration of EMI and UAV-based multispectral data, as highlighted by Guan *et al.* (2022), enhances the ability to predict soil properties by capturing fine-scale spatial variability. Their random forest models combining geophysical and spectral indices achieved high accuracy (R^2 = 0.87 for soil water content, R^2 = 0.91 for electrical conductivity). Our results mirror these findings, with ECa patterns strongly influenced by both soil texture and moisture content. The clay western zone, characterised by high ECa values, aligns with increased water retention and ionic concentrations, whereas the sand eastern zone, with lower ECa, corresponds to reduced water-holding capacity soils.

Our findings underscore the utility of integrating EMI and ERT data for textural mapping in vineyards and support the predictive frameworks proposed by Guan *et al.* (2022). These insights highlight the potential of hybrid geophysical-remote sensing approaches in precision viticulture and environmental management.

3. Correlation between leaf traits and apparent electrical conductivity

Nitrogen (Verdenal *et al.*, 2021) and water content (van Leeuwen *et al.*, 2009) in grapevine leaves are critical determinants of berry chemistry composition and

physiological functioning. This section investigates the potential of electrical conductivity (ECa) measurements as a relevant non-invasive proxy for these specific leaf traits, with the aim of improving understanding of plant–soil interactions and guiding precision viticulture practices.

Effectively, ECa reflects several soil properties, including moisture content, temperature, salinity, and texture (Corwin & Lesch, 2005). In viticultural systems, ECa measurements have been successfully employed to delineate spatial variability in soil characteristics and assess their influence on vine performance (Yu & Kurtural, 2020). Among these properties, soil moisture plays a central role: higher water content enhances ionic mobility, thereby increasing conductivity. Deep ECa measurements have shown strong correlations with vine water status indicators, such as stem water potential and stomatal conductance (Yu *et al.*, 2021).

While nitrogen content itself is not directly measurable with ECa, its availability and uptake are modulated by soil moisture and texture, both factors to which ECa is sensitive. Moist soils promote nitrogen mineralisation and enhance nutrient mobility, and variations in soil texture influence both water retention and nutrient dynamics, indirectly linking ECa to nitrogen status in the vine (Rodriguez-Perez *et al.*, 2011). Hence, ECa may serve as an integrative indicator of soil conditions that affect nutrient uptake.

To assess these relationships, we analysed the correlation between leaf traits (nitrogen, potassium, carbon, and water content) and ECa measurements of the soil at six investigation depths. Leaf trait values derived from spatial high-resolution hyperspectral drone imagery and averaged over a 1 m^2 grid centred on ECa measurement points to ensure consistency.

Nitrogen content in leaves exhibited limited variability across the study site (30–33 %), consistent with the relatively homogeneous phenological stage of sampled vines. In contrast, ECa values ranged from 1 to 42 mS/m, suggesting marked spatial variability in subsurface conditions.

When considering the entire dataset, no significant correlations were found between ECa and nitrogen content (Figure 6). However, stratification by soil texture revealed more nuanced relationships showing significant correlations were found between ECa and nitrogen content, with R^2 exceeding 0.4 in most channels, except the shallowest VCP 0.32 m channel, which was dominated by noise (Figure 7). The noise in this channel is partly due to statistical errors (less than 2 %) but is primarily caused by tillage from agricultural machinery affecting the top 0.30 m, which increases the soil's natural heterogeneity. These findings suggest that soil heterogeneity strongly influences the relationship between nitrogen uptake and subsurface conductivity.

Water content in leaves showed stronger and more consistent correlations with HCP configurations probing deeper subsurface layers (0.71 m and 1.18 m; $R^2 > 0.35$). These results align with existing literature on the sensitivity of ECa to soil moisture in vineyards (Yu & Kurtural, 2020), and further support the use of high depth of investigation of ECa measurements as indicators of vine water status, particularly in heterogeneous soils with variable water retention capacities. All correlation coefficients are summarised in Table 1.

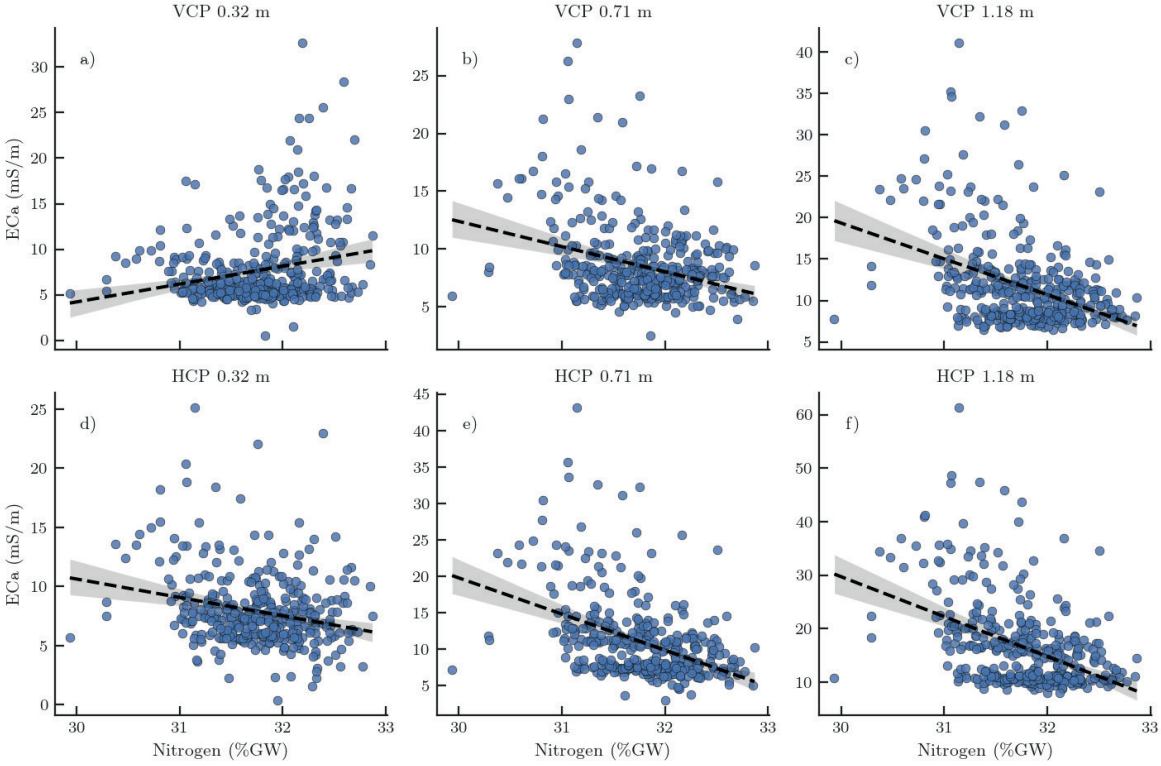


FIGURE 6. Correlation between leaf nitrogen content (drone-derived) and ECa across VCP (a to c) and HCP (d to f) configurations for three coil separations. The dashed line represents the linear regression.

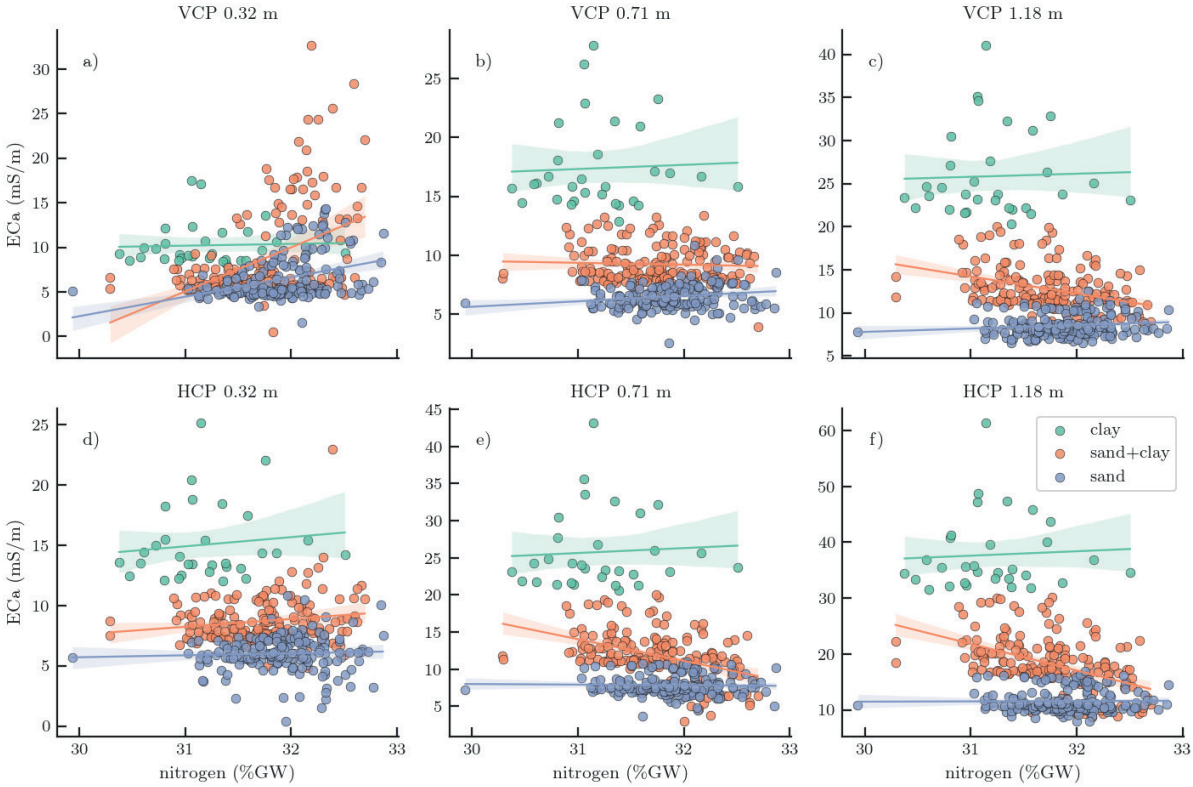


FIGURE 7. Correlation between nitrogen content and ECa values stratified by soil texture (clay, transition zone, sand). Linear regressions are shown for each group.

Correlations between ECa and potassium or carbon content were generally weak or non-significant (Table 1). Potassium showed occasional moderate correlations in the transition zone, but no consistent patterns were observed. Similarly, carbon content exhibited negligible correlations across soil classes. These results suggest that other factors, such as soil cation exchange capacity (CEC) or organic matter distribution, may be more directly linked to these leaf traits and should be considered in future models.

To validate the observed relationships, we used random forest regression to compare ECa-derived predictions with field-measured leaf traits at sampling locations. The model was trained using leave-one-out cross-validation to prevent overfitting by ensuring that its accuracy is evaluated on data it was not trained on. Significant correlations were observed between ECa and nitrogen content in 2022 (R^2 = 0.56) and between ECa and water content in 2023 (R^2 = 0.49), showing a trend between ECa, water, and nitrogen content (Figure 8). However, no significant correlations were detected for nitrogen content in 2023 or water content in 2022, highlighting interannual variability.

This variability likely stems from differences in data acquisition methods, soil natural heterogeneity, and meteorological conditions. ECa is dependent on water content, soil texture, and structure, as well as the measurement's volume of integration. In 2022, manual ECa measurements with lower spatial resolution were used, whereas continuous acquisition was employed in 2023. Additionally, rainfall differed significantly between the two years (118.5 mm in June 2022 *vs* 64.5 mm in June 2023), influencing water availability and nitrogen dynamics. Water content also exhibited a broader range in 2023 (63–72 %) compared to 2022 (67–69 %), potentially due to differing phenological stages and environmental conditions. All these parameters make it challenging to distinguish between the various contributing factors.

These findings demonstrate the potential of ECa data as a valuable tool for characterising key vine traits such as nitrogen and water content, under specific conditions. Stratifying data by soil texture and targeting deeper subsurface layers can improve the reliability of predictions. However, interannual variability and site-specific conditions must be carefully accounted for through standardised acquisition protocols and robust calibration efforts.

Further research should explore the mechanistic links between soil conductivity, nutrient availability, and plant uptake. Additionally, incorporating temporal data and expanding sampling across diverse soil types could improve model robustness and inform precision agriculture practices in viticulture.

4. Correlation between leaf water and nitrogen content and pseudo-3D EMI inversion

The fact that there is a fundamental distinction between inverted EC and ECa allows EC to be directly interpreted in terms of depth-specific soil properties (*i.e.*, texture, porosity), which is not feasible with ECa alone.

TABLE 1. Correlation values between ECa from different coil configurations and leaf components modelled from the drone-borne hyperspectral dataset, considering the soil type groups. No asterisk indicate a *p*-value greater than 0.05; one, two, and three asterisks indicate *p*-values smaller than 0.05, 0.01, and 0.001, respectively.

	VCP 0.32 m	VCP 0.71 m	VCP 1.18 m	HCP 0.32 m	HCP 0.71 m	HCP 1.18 m
Water						
All data	0.04	0.21***	0.21***	0.14**	0.19***	0.19***
Clay	0.4*	0.42*	0.41*	0.42*	0.39*	0.37*
Sand + clay	0.24**	–0.11	–0.3***	0.06	–0.31***	–0.32***
Sand	0.13	0.08	–0.07	–0.26***	–0.17*	–0.17*
Potassium						
All data	0.15**	–0.07	–0.14**	–0.09	–0.16**	–0.17***
Clay	–0.03	–0.02	–0.03	–0.09	–0.05	–0.07
Sand + clay	–0.13	0.1	0.22**	0	0.23**	0.22**
Sand	–0.09	–0.06	–0.17*	–0.23	–0.19**	–0.22**
Carbon						
All data	–0.05	0.02	0.06	0.05	0.08	0.09
Clay	0	0.03	0.03	0.09	0.06	0
Sand + clay	–0.13	0.1	0.22**	0	0.23**	0.22**
Sand	0.02	0	0.14	0.19**	0.19**	0.21**
Nitrogen						
All data	0.23***	–0.32***	–0.4***	–0.24***	–0.43***	–0.44***
Clay	0.04	0.05	0.03	0.12	0.06	0.06
Sand + clay	0.44***	–0.05	–0.37***	0.16*	–0.43***	–0.46***
Sand	0.38***	0.19**	0.13	0.05	–0.03	0.01

One key advantage of using pseudo-3D inverted EC is its ability to characterise vertical variations in soil properties and assess their influence on plant physiological responses. In this section, we investigate the potential of pseudo-3D inverted EC to provide insights into leaf constituents by evaluating its correlation with leaf water and nitrogen content at varying depths. The primary objective is to identify subsurface zones that interact with and potentially influence vine functional traits, with implications for vineyard management and precision viticulture.

The pseudo-3D inversion of ECa data allowed for a detailed examination of the relationship between EC and leaf water content as a function of depth. Two primary findings emerge from this analysis:

– Limited improvement over ECa in correlation strength: the use of pseudo-3D inverted EC did not significantly enhance the overall correlation scores compared to ECa. This result highlights that ECa, being simpler and faster to measure in the field, remains a valuable tool for studying plant–soil interactions. However, its integrated nature precludes depth-specific interpretation, which is critical for understanding root-zone processes; and
– Depth-specific correlations reveal functionally relevant soil layers: the primary advantage of pseudo-3D inverted EC emerges when analysing correlation profiles as a function of depth. As shown in Figure 9, the correlation between EC and leaf water content increases with depth, stabilising around 0.5 m. Beyond this threshold, the inverted EC shows significant correlations ($R2 > |0.55|$) with both leaf nitrogen content in 2022 (blue line) and leaf water content in 2023 (orange line). These results suggest that the root system predominantly concentrated around 0.5 m in the study area, making this layer particularly relevant for interpreting soil–plant interactions.

These depth-resolved correlations also help explain the lack of significant correlations observed at shallower depths. For instance, at 30 cm, no meaningful relationships were detected between soil water content, leaf water content, and ECa. This suggests that the geophysical signal at this depth does not adequately capture the subsurface conditions most relevant to vine physiology, which appear to be influenced by deeper soil layers, where root water and nutrient uptake are more active.

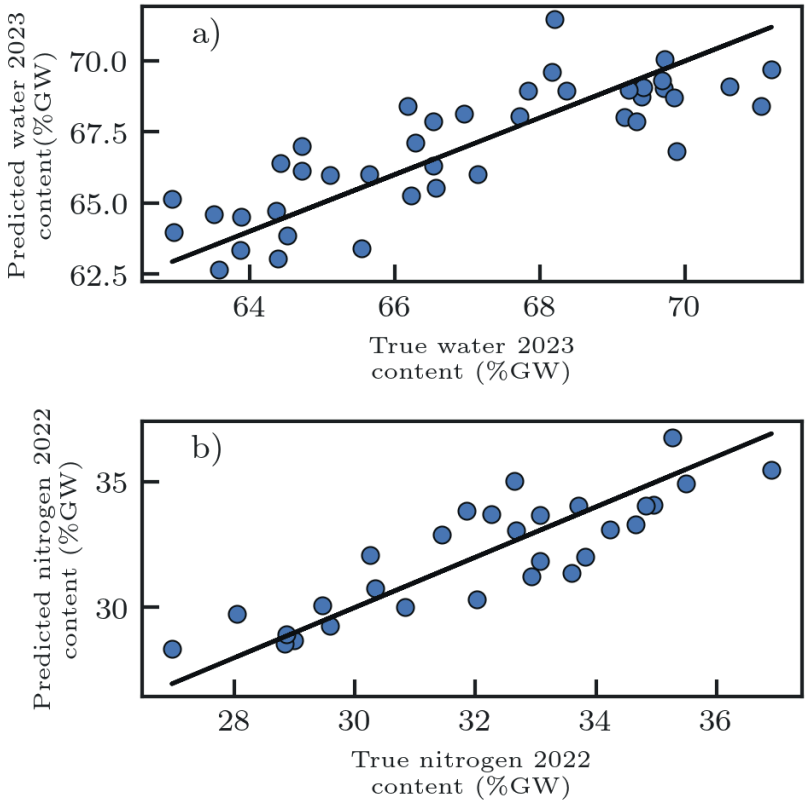


FIGURE 8. Random forest regression results for leaf water content (2023, 45 locations) and nitrogen content (2022, 30 locations), predicted from ECa data. Panels show the a) water content and b) nitrogen content.

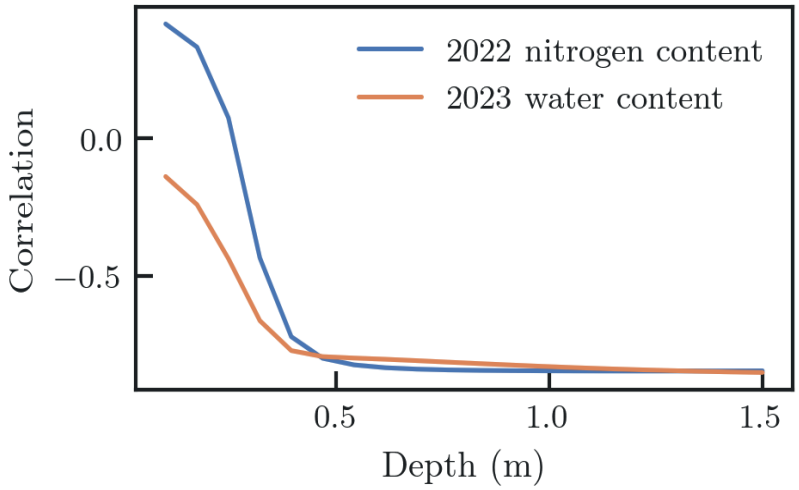


FIGURE 9. 3D EMI inversion results correlated with depth. Correlation between leaf traits and 3D inverted EC as a function of depth. The blue curve represents leaf nitrogen content in 2022, while the orange curve represents leaf water content in 2023.

Thus, while pseudo-3D inverted EC may not always outperform ECa in terms of global correlation strength, it offers critical added value by providing depth-specific information. This allows for the identification of key soil horizons influencing vine function and the potential conversion of EC values into meaningful physical parameters such as soil texture and structure. Such capabilities are essential for improving our understanding of vine responses to soil heterogeneity and for informing site-specific management practices in viticulture.

5. Integrating hyperspectral and geophysical data

The observed spatial patterns emphasise the necessity of integrating hyperspectral imaging with geophysical methods to better capture the interplay between soil characteristics and plant responses. As shown in Yu and Kurtural (2020), random forest models effectively link hyperspectral and geophysical data, enabling interpretable relationships between spectral signatures and soil properties.

Our results similarly demonstrate the advantages of raw spectral data over index-based approaches, particularly in heterogeneous vineyard environments.

By accounting for variations in soil texture, drainage, and plant development stages, specific machine learning models proved more accurate than generalised ones. This aligns with Yu and Kurtural (2020)'s findings and highlights the value of targeted, data-driven approaches for addressing complex soil–plant interactions. While hyperspectral imaging provides fine-scale information on leaf traits, geophysical data such as soil electrical conductivity offer insights into underlying soil processes. Together, these tools enable a holistic understanding of vineyard variability, supporting precision interventions that optimise water and nutrient management.

6. Synthesis

In 2022, a complete dataset was acquired, including EMI, ERT, soil samples, hyperspectral data (both drone- and hand-based), and leaf samples (Table 2a). The collected leaves were carefully selected to ensure a homogeneous physiological and health status across samples.

In contrast, the 2023 campaign exhibited several methodological and phenological differences despite identical measurement dates. Due to technical and budget constraints, no drone-based hyperspectral data were acquired (Table 2b). Additionally, a broader range of leaf samples was intentionally collected, including leaves exhibiting diverse health and developmental conditions, to assess the impact of plant variability on the relationships investigated. EMI data in 2023 were acquired in continuous mode along the exact same transects as in 2022 to evaluate the repeatability of the results despite differences in acquisition mode and plant status.

A major distinction between the two campaigns lies in the phenological stage of the grapevines. In 2022, measurements were conducted close to the flowering period, whereas in 2023, the vines were in the berry growth stage. This phenological shift is likely to have influenced the relationships observed between geophysical, hyperspectral, and leaf physiological parameters.

The contributions of each method with the best correlation indexes to characterise leaf traits are summarised in Table 2. Notably, in 2022, apparent electrical conductivity (ECa) and inverted EC emerged as the most effective predictors of leaf nitrogen content (R^2 = 0.68 for ECa and R^2 = 0.80 for inverted EC), surpassing both hand-held (R^2 = 0.65) and drone-based (R^2 = 0.64) hyperspectral indices. This finding suggests that under specific conditions, potentially linked to the flowering stage, geophysical methods may offer superior predictive power for leaf nitrogen status. However, these conditions warrant further investigation, as geophysical indicators showed no predictive capability for leaf nitrogen in 2023, possibly due to differences in phenological stage, rainfall, or other environmental factors.

Interestingly, the relationship between geophysical data and leaf water content followed an inverse pattern. In 2022, ECa and inverted EC failed to predict leaf water content, despite their well-documented effectiveness in assessing soil water status (*e.g.*, van Leeuwen *et al.*, 2024; and references therein). In contrast, in 2023, leaf water content was reliably predicted by all methods employed ($R^2 \geq 0.74$), ECa, inverted EC, and the hand-held spectrometer, suggesting that the relevance of each method may shift according to the phenological development of the vine. In 2023, no other plant feature (carbon, nitrogen, or potassium) could be detected: with very low correlation for the hand spectrometer ($R^2 \leq 0.5$), and no correlation at all with geophysics (ECa and inverted EC).

These contrasting results lead to the hypothesis that geophysical methods may be particularly suitable for nitrogen status assessment around the flowering stage, whereas water status might be more effectively characterised during berry development. This temporal dependence underscores the necessity of aligning measurement strategies with vine phenology to optimise diagnostic accuracy, which is a point that merits further dedicated study.

TABLE 2. Synthesis of the best correlation coefficient between each method (hand-spectrometer, drone-based spectrometer, ECa, and inverted EC) and leaf component (nitrogen, carbon, potassium, water content) for: a) the 2022 campaign, and b) the 2023 campaign. *: corresponds to *p*-value < 0.05, **: corresponds to *p*-value < 0.01, and ***: corresponds to *p*-value < 0.001.

2a) Correlations 2022	Carbon %	Nitrogen %	Water %	Potassium %
Hand-based spectrometer	0.54**	0.65***	–0.42*	0.57**
Drone-based spectrometer	–0.61***	0.64***	–0.5**	0.5**
Pseudo-3D EC inversion		–0.84***		
ECa		0.68**		
2b) Correlations 2023	**Carbon %**	**Nitrogen %**	**Water %**	**Potassium %**
Hand spectrometer	0.3*	0.33*	0.8***	0.5*
3D inversion			–0.85***	
ECa			–0.74***	

It is also important to note that other experimental factors may have contributed to the observed variability between years. Differences in EMI acquisition resolution, leaf sampling strategies (homogeneous in 2022 *versus* intentionally variable in 2023), and the inclusion of new characterisation points in 2023 could have influenced the outcomes.

In summary, these findings highlight the complex interplay between vine phenology, measurement protocols, and environmental conditions in determining the effectiveness of geophysical and hyperspectral methods for assessing leaf physiological traits. Future research should aim to refine these relationships to enable more reliable, stage-specific recommendations for vineyard monitoring.

CONCLUSION

This study highlights the feasibility of integrating airborne hyperspectral imaging and geoelectrical measurements for effective monitoring of soil and plant health in vineyards. Although direct correlations between leaf traits and apparent electrical conductivity (ECa) were modest, integrating soil texture clustering significantly improved data interpretation, demonstrating the complementary strengths of geophysical and hyperspectral methodologies. The comprehensive investigations conducted over the years 2022 and 2023 included a wide array of measurements such as EMI, hyperspectral imaging, leaf and soil sampling, and spectrometer analyses, with progressive expansion in data acquisition and station coverage. Analytical techniques like EMI-ERT pseudo-3D inversion and soil texture clustering allowed for robust exploration of the relationships between soil, plant, and geophysical parameters. Notably, hand-held spectrometer measurements showed a strong predictive relationship with leaf traits (R^2 = 0.8), and airborne hyperspectral data yielded similarly significant correlations.

A key finding was the variability in correlations between geophysical data and leaf traits across years, attributed to differences in weather conditions and vine phenology. For instance, nitrogen content in 2022 and water content in 2023 correlated strongly with inverted electrical conductivity (EC) at depths greater than 50 cm, pinpointing the depth of primary root system development. Conversely, the lack of correlation in other year-parameter combinations highlights the influence of acquisition modes and vine growth stages. Specifically, flowering occurred earlier in 2022 than in 2023, emphasising the importance of aligning acquisition timing with phenological phases when studying plant–soil interactions. Hand-held spectrometer data emerged as the most reliable tool for estimating plant components indirectly, offering minimal interference from atmospheric and shadow effects.

The study underscores the potential of integrating hyperspectral and geophysical datasets for precision viticulture. However, challenges remain. As noted by Peanusaha *et al.* (2024), environmental factors and sensor limitations can introduce variability in spectral data. Similarly, Guan *et al.* (2022) highlighted the need to address temporal mismatches between geophysical and UAV data acquisition. In the present study, differences in phenological stages and sampling strategies between 2022 and 2023 likely contributed to the observed variability, reinforcing the necessity of tailored protocols according to vine development phases. Future research should focus on developing hybrid models that combine spectral and geophysical data, utilising machine learning techniques to enhance predictive accuracy. In particular, incorporating SWIR bands sensitive to protein content, as suggested by Peanusaha *et al.* (2024), could improve nitrogen estimation. Additionally, exploring the effects of soil water content and texture on nutrient uptake, as recommended by Guan *et al.* (2022), could further refine the methodologies and interpretations presented here. Moreover, the differential predictive power of geophysical and hyperspectral methods depending on vine phenological stages suggests that adaptive, season-specific monitoring frameworks could optimise resource allocation and data quality in vineyard management.

Importantly, our results suggest that geophysical methods may be more effective than hyperspectral imaging for characterising leaf nitrogen content, especially considering that airborne hyperspectral data can be costly, complex to process, and dependent on soil homogeneity, conditions that can be more readily characterised through geophysics. In contrast, traits such as leaf carbon and potassium were better assessed using hyperspectral data. Leaf water content may also be accessible through geophysics, though further research is needed to clarify this relationship in relation to vine growth stages. While hand-held hyperspectral instruments demonstrated strong local reliability, they are not suitable for whole-plot characterisation. Drone-based hyperspectral imaging offers broader integration potential, but at the expense of high acquisition costs and processing complexity requiring advanced expertise. Therefore, a multi-scale approach combining local (hand-held) and plot-scale (geophysical and drone) data could offer a pragmatic balance between precision and operational feasibility. Further validation across different plots, seasons, and years is necessary to confirm these findings.

In conclusion, this study represents one of the first comprehensive efforts to combine geophysical and hyperspectral data for vineyard applications. The findings highlight the potential of geophysical techniques to infer internal leaf compositions and establish links between soil heterogeneity and plant performance. This work lays the groundwork for advancing pedophysical models that integrate soil and plant parameters, enabling a more nuanced understanding of plant–soil interactions. Ultimately, these insights pave the way for precision viticulture tools capable of real-time, stage-specific monitoring, improving both agronomic decision-making and environmental sustainability. Future research should aim to expand datasets, refine methodologies, and explore additional depths, spatial resolutions, and phenological stages to further enhance the predictive capabilities of these integrated approaches.

ACKNOWLEDGEMENTS

This work was supported by the Institut Carnot ISIFOR. The authors thank Baptiste Dafflon for his valuable review, helping to improve the manuscript.

REFERENCES

Ammoniaci, M., Kartsiotis, S. P., Perria, R., and Storchi, P. (2021). State of the art of monitoring technologies and data processing for precision viticulture. *Agriculture*, *11*(3), 201. https://doi.org/10.3390/agriculture11030201

Anderson, M. C., Neale, C. M. U., Li, F., Norman, J. M., Kustas, W. P., Jayanthi, H., Chavez, J. (2004). Upscaling ground observations of vegetation water content, canopy height, and leaf area index during SMEX02 using aircraft and Landsat imagery. *Remote Sensing of Environment*. https://doi.org/10.1016/j.rse.2004.03.019

Berger, K., Verrelst, J., Feret, J.B., Hank, T., Wocher, M., Mauser, W., Camps-Valls, G. (2020). Retrieval of aboveground crop nitrogen content with a hybrid machine learning method. *Int. J. Appl. Earth Obs*. Geoinf. 92 (April), 102174 https://doi.org/10.1016/j.jag.2020.102174

Bonfante, A., Agrillo, A., Albrizio, R., Basile, A., Buonomo, R., De Mascellis, R., Gambuti, A., Giorio, P., Guida, G., Langella, G., Manna, P. Minieri, L., Moio, L., Siani, T.. Terribile, F. (2015). Functional homogeneous zones (fHZs) in viticultural zoning procedure: An Italian case study on Aglianico vine. *Soil*. https://doi.org/10.5194/soil-1-427-2015

Brevik, Eric C., Calzolari, C. Bradley, A., Miller, Pereira, P., Kabała, C., Baumgarten, A., Jordán, A. (2016). Soil Mapping, Classification, and Pedologic Modeling: History and Future Directions, *Geoderma*, 264, 256-274. https://doi.org/10.1016/j.geoderma.2015.05.017

Cavender-Bares, J., Gamon, J. A., & Townsend, P. A. (2020). *Remote sensing of plant biodiversity* (p. 581). Springer Nature. https://doi.org/10.1007/978-3-030-33157-3

Chadwick, K. D., Brodrick, P. G., Grant, K., Goulden, T., Henderson, A., Falco, N., Wainwright, H., Williams, K. H., Bill, M., Breckheimer, I., Brodie, E. L., Steltzer, H., Rick Williams, C. F., Blonder, B., Chen, J., Dafflon, B., Damerow, J., Hancher, M., Khurram, A., … Maher, K. (2020). Integrating airborne remote sensing and field campaigns for ecology and Earth system science. Methods in Ecology and Evolution. https://doi.org/10.1111/2041-210X.13463

Corwin, D. L., and Lesch, S. M. (2005). Apparent soil electrical conductivity measurements in agriculture. *Computers and electronics in agriculture*, *46*(1-3), 11-43. https://doi.org/10.1016/j.compag.2004.10.005

Darra, N., Psomiadis, E., Kasimati, A., Anastasiou, A., Anastasiou, E., and Fountas, S. (2021). Remote and proximal sensing-derived spectral indices and biophysical variables for spatial variation determination in vineyards. *Agronomy*, *11*(4), 741. https://doi.org/10.3390/agronomy11040741

Das, B. S., Ray, S., Sarathjith, M. C., Santra, P., Sahoo, R. N., Srivastava, R. (2015). Hyperspectral remote sensing: Opportunities, status and challenges for rapid soil assessment in india hyperspectral remote sensing: Opportunities, status and challenges for rapid soil assessment in India. *Current Science*, 108(5), 860–868.

Doolittle, J.A., Sudduth, K.A., Kitchen, N.R., Indorante, S.J. (1994). Estimating depth to claypans using electromagnetic inductive methods. *J. Soil Water Conserv*. 49:552-555. https://doi.org/10.1080/00224561.1994.12456905

Ferraty, F., and Vieu, P. (2006). Functional nonparametric statistics in action. In *The art of semiparametrics* (pp. 112-129). Heidelberg: Physica-Verlag HD. https://doi.org/10.1007/3-7908-1701-5_8

Fuentes, S., and Gago, J. (2022). Modern approaches to precision and digital viticulture. In *Improving sustainable viticulture and winemaking practices* (pp. 125-145). Academic Press. https://doi.org/10.1016/B978-0-323-85150-3.00015-3

Ge, Y., Atefi, A., Zhang, H., Miao, C., Ramamurthy, R.K., Sigmon, B., Yan, J., Schnable, J.C. (2019). High-throughput analysis of leaf physiological and chemical traits with VIS–NIR–SWIR spectroscopy: a case study with a maize diversity panel. *Plant Methods* 15, 66, https://doi.org/10.1186/s13007-019-0450-8

Grote, K., Anger, C., Kelly, B., Hubbard, S., & Rubin, Y. (2010). Characterization of soil water content variability and soil texture using GPR groundwave techniques. *Journal of Environmental & Engineering Geophysics*, 15(3), pp.93-110. https://doi.org/10.2113/JEEG15.3.93

Guan, Y., Grote, K., Schott, J., & Leverett, K. (2022). Prediction of soil water content and electrical conductivity using random forest methods with UAV multispectral and ground-coupled geophysical data. *Remote Sensing*, *14*(4), 1023. https://doi.org/10.3390/rs14041023

Henrich, V., Krauss, G., Götze, C., Sandow, C. (2012). IDB - www.indexdatabase.de, Entwicklung einer Datenbank für Fernerkundungsindizes. AK Fernerkundung, Bochum, 4.-5. 10. 2012.

Hubbard, S. S., Schmutz, M., Balde, A., Falco, N., Peruzzo, L., Dafflon, B., Léger, E., Wu, Y. (2021). Estimation of Soil Classes and Their Relationship to Grapevine Vigor in a Bordeaux Vineyard: Advancing the Practical Joint Use of Electromagnetic Induction (EMI) and NDVI Datasets for Precision Viticulture, *Precision Agriculture*, 22, 1353-1376. https://doi.org/10.1007/s11119-021-09788-w

Jacquemoud, S., and Ustin, S. (2019). *Leaf optical properties*. Cambridge University Press. https://doi.org/10.1017/9781108686457

Johnson, L. F., Roczen, D. E., Youkhana, S. K., Nemani, R. R., Bosch, D. F. (2003). Mapping vineyard leaf area with multi-spectral satellite imagery. *Computer and Electronics in Agriculture*, 38, 33–44. https://doi.org/10.1016/S0168-1699(02)00106-0

Lamsal, K., Malenovský, Z., Woodgate, W., Waterman, M., Brodribb, T. J., & Aryal, J. (2022). Spectral Retrieval of Eucalypt Leaf Biochemical Traits by Inversion of the Fluspect-Cx Model. *Remote Sens. 14*, 567. https://doi.org/10.3390/rs14030567

Loke, M.H. (2004). Tutorial: 2-D and 3-D Electrical Imaging Surveys. Geotomo Software, Res2dinv 3.5 Software.

Martini, E., Comina, C., Priori, S., and Costantini, E. A. C. (2013). A combined geophysical-pedological approach for precision viticulture in the Chianti hills. *Bollettino di Geofisica Teorica ed Applicata*, *54*(2).

McLachlan, P., Schmutz, M., Cavailhes, J., & Hubbard, S. (2022). Estimating grapevine-relevant physicochemical soil zones using apparent electrical conductivity and in-phase data from EMI methods. *Geoderma*. https://doi.org/10.1016/j.geoderma.2022.116033

McLachlan, P., Blanchy, G., & Binley, A. (2021). Emagpy: Open-source Standalone Software for Processing, Forward Modeling and Inversion of Electromagnetic Induction Data, *Computer and Geosciences*, 146, 104561. https://doi.org/10.1016/j.cageo.2020.104561

McNeill, J. D. (1980). Electrical conductivity of soils and rocks. Mississauga, Ontario, Canada: Geonics Limited.

Moghimi, A., Pourreza, A., Zuniga-Ramirez, G., Williams, L.E., and Fidelibus, M.W. (2020). A novel machine learning approach to estimate grapevine leaf nitrogen concentration using aerial multispectral imagery. *Remote Sensing*, 12(21), p.3515. https://doi.org/10.3390/rs12213515

NF EN ISO 16634-2. (2016). Détermination de la teneur en azote total par combustion selon le principe Dumas et calcul de la teneur en protéines brutes. 34p.

NF EN ISO 662. (2001). Détermination de la teneur en eau et en matières volatiles. 12p.

NF X31-107. (2003). Détermination de la distribution granulométrique des particules du sol. 20p.

Ordóñez, C., Rodríguez-Pérez, J. R., Moreira, J., Sanz, E. (2013). Using Hyperspectral Spectrometry and Functional Models to Characterize Vine-Leaf Composition. *IEEE* Xplore, 51, 5. https://doi.org/10.1109/TGRS.2012.2217344

Peanusaha, S., Pourreza, A., Kamiya, Y., Fidelibus, M. W., & Chakraborty, M. (2024). Nitrogen retrieval in grapevine (Vitis vinifera L.) leaves by hyperspectral sensing. *Remote Sensing of Environment*. Mar 1;302:113966. https://doi.org/10.1016/j.rse.2023.113966

Pradipta, A., Soupios, P., Kourgialas, N., Doula, M., Dokou, Z., Makkawi, M., ... and Yassin, M. (2022). Remote sensing, geophysics, and modeling to support precision agriculture—Part 1: Soil applications. *Water*, *14*(7), 1158. https://doi.org/10.3390/w14071158

Pugnaire, F.I., Morillo, J., Peñuelas, J., Reich, P., Reich, P. Bardgett, R., Gaxiola, A., Wardle, D., van der Putten, W. (2019). Climate Change Effects on Plant-Soil Feedbacks and Consequences for Biodiversity and Functioning of Terrestrial Ecosystems, *Science Advances*, 5, 11. https://doi.org/10.1126/sciadv.aaz1834

Revil, A., Schmutz, M., Abdulsamad, F., Balde, A., Beck, C., Ghorbani, A. Hubbard, S.S. (2021). Field-scale estimation of soil properties from spectral induced polarization tomography. *Geoderma*, 403, p.115380. https://doi.org/10.1016/j.geoderma.2021.115380

Rodríguez-Pérez, J. R., Plant, R. E., Lambert, J. J., and Smart, D. R. (2011). Using apparent soil electrical conductivity (EC a) to characterize vineyard soils of high clay content. *Precision Agriculture*, *12*, 775-794. https://doi.org/10.1007/s11119-011-9220-y

Sarri, D., Martelloni, L., Rimediotti, M., Lisci, R., Lombardo, S., and Vieri, M. (2019). Testing a multi-rotor unmanned aerial vehicle for spray application in high slope terraced vineyard. *Journal of Agricultural Engineering*, *50*, 38-47. https://doi.org/10.4081/jae.2019.853

Triantafilis, J. and Lesch, S.M. (2005). Mapping clay content variation using electromagnetic induction techniques. *Computers and Electronics in Agriculture*, 46(1-3), pp.203-237. https://doi.org/10.1016/j.compag.2004.11.006

Ustin, S.H., Gitelson, A.A., Jacquemoud, S., Schaepman, M., Asner, G.P., Gamon, J.A., Zarco-Tejada, P. (2009). Retrieval of foliar information about plant pigment systems from high resolution spectroscopy. *Remote Sensing of Environment*, Volume 113, Supplement 1, S67-S77, ISSN 0034-4257. https://doi.org/10.1016/j.rse.2008.10.019

van Leeuwen, C. (2021). The use of near surface geophysics to estimate soil related terroir factors in viticulture. In *NSG2021 2nd Conference on Geophysics for Infrastructure Planning, Monitoring and BIM* (Vol. 2021, No. 1, pp. 1-5). European Association of Geoscientists & Engineers. https://doi.org/10.3997/2214-4609.202120234

van Leeuwen, C., Schmutz, M., & de Rességuier, L. (2024). The contribution of near surface geophysics to measure soil related terroir factors in viticulture: a review. *Geoderma*. https://doi.org/10.1016/j.geoderma.2024.116983

van Leeuwen, C., Trégoat, O., Choné, X., Bois, B., Pernet, D., & Gaudillère, J. P. (2009). Vine water status is a key factor in grape ripening and vintage quality for red Bordeaux wine. How can it be assessed for vineyard management purposes?. *Oeno One*, *43*(3), pp.121-134. https://doi.org/10.20870/oeno-one.2009.43.3.798

Verdenal, T., Dienes-Nagy, Á., Spangenberg, J.E., Zufferey, V., Spring, J.L., Viret, O., Marin-Carbonne, J., and Van Leeuwen, C. (2021). Understanding and managing nitrogen nutrition in grapevine: A review. *Oeno One*, *55*(1), pp.1-43. https://doi.org/10.20870/oeno-one.2021.55.1.3866

Yu, R. and Kurtural, S.K. (2020). Proximal sensing of soil electrical conductivity provides a link to soil-plant water relationships and supports the identification of plant water status zones in vineyards. *Frontiers in Plant Science*, 11, p.244. https://doi.org/10.3389/fpls.2020.00244

Yu, R., Zaccaria, D., Kisekka, I., and Kurtural, S. K. (2021). Soil apparent electrical conductivity and must carbon isotope ratio provide indication of plant water status in wine grape vineyards. *Precision Agriculture*, *22*(4), 1333-1352. https://doi.org/10.1007/s11119-021-09787-x